Montanuniversität Leoben

Antibacterial films for medical applications grown by atmospheric pressure plasma deposition

Diploma Thesis

Elisabeth Jäger

Jena/Leoben, March 2014

Affidavit

I declare in lieu of oath, that I wrote this thesis and performed the associated research myself, using only literature cited in this volume.

Jena/Leoben, March 2014

Acknowledgement

Contents

List of abbreviations

MDD   Medical device directive

Cu   Copper

Zn   Zinc

ZnO   Zinc oxide

APCVD   Atmospheric pressure chemical vapour deposition

CVD   Chemical vapour deposition

HMDSO   Hexamethyldisiloxane

PVD   Physical vapour deposition

DNA   Deoxyribonucleic acid

NP   Nanoparticles

DC   Direct current

$Cu(NO_3)_2$ Copper nitrate

$Zn(NO_3)_2$ Zinc nitrate

SiO_X Silicon oxide

Ra   Average roughness

SEM   Scanning electron microscopy

EDX   Energy dispersive X-ray spectroscopy

XPS   X-ray photoelectron spectroscopy

AFM   Atomic force microscopy

MC 3T3-E1   Mouse cells

EDTA   Ethylene diaminetetraacetic acid

PBS   Phosphate buffered saline

FDA   Fluoreszeindiacetat

BTG   BacTiter-Glo

E. coli   Escherichia coli

1 Theoretical aspects

1.1 Introduction

The goal of this work is to produce and characterise an antiseptic film for medical applications grown by atmospheric pressure plasma chemical vapour deposition.

First, a short introduction of wounds and the healing process is given; this is followed by a summary of requirements for implants and medical devices. The legal basis, which is defined in the medical device directive [1], is further discussed as an important prerequisite for experimental studies for medical applications. As next, a brief description of the antibacterial active agents copper and zinc and their antibacterial ability is given. Finally, the state of the art of atmospheric pressure chemical vapour deposition as the deposition process used in this thesis is introduced.

1.2 Wounds, implants and medical instruments

The most common injury in Austria is a femoral fracture usually happening during hiking or skiing. In the case of complicated injuries a timely surgery is necessary. Surgical nails, screws and plates are commonly used to fix the fractured bone to ensure a successful healing process. In the next paragraph the wound healing mechanisms are discussed, as well as the requirements for implants and medical instruments.

1.2.1 Wound healing

A wound is a specific type of injury, in which skin is torn, cut or punctured, or where blunt force trauma causes a contusion [2]. There are mechanically caused wounds, with both sharp and blunt force, as well as thermal, radiogenic and chemical wounds. Further, mechanically caused wounds such as open or surgical wounds are known.

The human body can sustain a variety of injuries, because of a very efficient healing mechanism, characterized by four distinct but overlapping phases: haemostasis, inflammation, proliferation and remodelling.

At the time of injury, the tissue is disrupted and blood components spill into the wound. Platelets adhere to the exposed collagen and to each other. The platelets release clotting factors as well as essential growth factors and cytokines, to initiate the repair process. This part of wound healing is called haemostasis. Then neutrophils enter the wound site and begin to remove foreign materials, bacteria and damaged tissue. In the inflammation phase

the macrophages appear and continue the process of cleaning out the wound, as well as they recruit fibroblasts to the wound site. This is the beginning of the proliferative phase. The fibroblasts deposit new extracellular matrix. Then new collagen matrix becomes cross-linked and organized during the final remodelling phase. This phase is characterized by continued synthesis and degradation of the extracellular matrix components trying to establish a new equilibrium [3].

This mechanism explains the most important response following a tissue injury. But three other possible responses are well known: excessive healing, deficient healing and regeneration. In excessive healing there is too much deposition of connective tissue that results in altered structure and thus loss of functionality. Deficient healing exists when there is an insufficient deposition of connective tissue matrix and the tissue is weakened to the point where it can fall apart [3]. It has been observed that humans lose the ability of regeneration, which is a process to replace the damaged structure and re-establish its functionality as it was before the injury. A typical example is the human liver which can be effectively regenerated after injury.

Deficient healing and excessive healing are pathological responses to injury leading to fibrosis or chronic ulcers, which may occur if any part of the healing sequence is altered, for example by microorganisms.

1.2.2 Requirements for implants and medical instruments

An implant is an artificial medical device to replace a missing biological structure, support a damaged biological structure or enhance an existing biological structure [4]. Three types of implants are well established: medical implants, plastic implants and functional implants. The most commonly used medical implants are artificial pacemaker, stents, dental implants and orthopaedic implants. In this study the focus is exclusively laid on orthopaedic implants and the associated medical instruments. There are two different types of implants, short-term implants and permanent implants. The short-term implants should not connate with the new tissue, whilst the permanent implants should be incorporated as soon as possible. Both have to be accepted by the body.

It is important to control properties of the implants and medical instruments, especially the antibacterial capability, mechanical properties and corrosion resistance. The products should show an antibacterial but no cytotoxic effect to protect the patient from microorganisms, which cause pathological responses to injury. They have to be robust and wear resistant. Furthermore, implants as well as medical instruments should be able to endure sterilisation.

As a general rule, implants must be readily available in sufficient quantity, especially in case of emergency. A very important requirement is also sustainability. The products should be easy to manufacture and the production should be environment-friendly. Furthermore, a high efficiency and reliability is required, which means the products have to work well and fulfil the desired requirements at a high level as well as perform within their specification for all environmental conditions and for a sufficiently long life time. Moreover, the products have to be affordable as mass products, both in initial investment and in operating terms. The last two important points are safety and acceptance. There are numerous regulations governing the safety of medical devices and pharmacological products. For human applications, whilst there is always a risk-benefit assessment, safety is the prime consideration. The products have to be generally acceptable both for practitioners and for the patients or the public. This includes ease of operation, synergetic design and an intuitive application processes [5].

1.3 Medical device directive

The rapid development of medical products required a harmonisation of law relating to medical devices within the European Union. The Medical device directive (MDD), or Council directive 93/42/EEC, entered into force fully on 14th July 1993. The last amendment was on 21st March 2010.

The MDD comprises a classification of medical devices and associated requirements. The medical device should provide patients with a high level of protection and attain the performance level attributed to them by the manufacturer. Therefore, the maintenance or improvement of the level of protection is one of the essential objectives of this directive [1]. Moreover, the MDD includes production, placing on the market, operation and application of medical devices.

1.3.1 Classification of medical devices

The classification of medical devices in the European Union is outlined in Annex IX of the MDD. There are basically four classes to estimate the risk of the patient due to applying a medical device.

The European classification depends on rules that involve the medical device's duration of body contact, invasive character, reusable medical instruments, active devices and the use of biological material from animals or human bodies. Some examples for the four classes are listed in the Tab. 1 [1]:

Table 1: Risk classes of medical devices [1]

Class	Examples
I	Wheelchairs, bandages, reusable medical devices
IIa	Disposable syringes, contact lenses, diagnostic ultrasonic devices
IIb	Blood bags, ventilators, dental implants
III	Hip, knee or shoulder replacements, pacemakers, stents

The risk for the patient is increasing from Class I to Class III. Therefore, the inspection effort of medical devices is increasing too. The testing ranges from simple tests to multi-years clinical studies of medical products.

1.3.2 Implants and medical instruments with active agents

General, there is no standard existing for implants and medical devices with active agents. The medical device directive distinguishes medical products with and without drugs. Neither copper nor zinc was treated as pharmaceutical product, but for this application they should be considered as active agents or drugs. Therefore, implants and medical instruments with active agents, produced for this work, can be attributed to Class III. Thus a medical study is necessary for market access, but this is always a lengthy and costly process. As long as the medical product is not certificated, the manufacturer is responsible for any damage.

1.4 Active agents

One possible solution for antiseptic surfaces is to dope the film with antiseptic elements. These are antimicrobial substances to reduce the possibility of infection, sepsis and putrefaction. In this study zinc and copper were used as active agents. Their physical and chemical properties are essential to explain the antiseptic effect.

1.4.1 Copper and its properties

Copper (Cu) is a metallic chemical element where the name comes from the Latin word cuprum. Copper has an atomic number of 29 and can be found in group 11 of the periodic table, together with silver and gold. All these elements have one s-orbital electron on top of a filled d-electron shell and are characterized by high ductility and electrical conductivity. Copper has a high thermal conductivity as well, which is the second highest among pure metals at room temperature [6].

Copper is also one of the metals with a natural colour other than grey or silver. Freshly exposed surface has a reddish-orange colour and acquires a reddish-tarnish, when exposed to the air as a consequence of oxidation [6]. Copper forms a rich variety of compounds with oxidation states +1 and +2.

1.4.2 Zinc and its properties

Zinc is a metallic chemical element, having the symbol Zn and the atomic number 30. Zinc is a member of group 12 of the periodic table. It is a moderately reactive metal and a strong reducing agent. The surface of the pure metal tarnishes quickly, forming a protective passivating layer [7].

Zinc is hard and brittle at most temperatures and it is a fair conductor of electricity. Zinc has a relatively low melting point of 419.5 °C [7].

The chemistry of zinc is dominated by the +2 oxidation state. A very common binary compound is zinc oxide, which is an inorganic compound with the formula ZnO. ZnO is a white powder that is insoluble in water, which is widely used as an additive in numerous materials and products including plastics, ceramics, glass, cement, lubricants, paints, adhesives, sealants, pigments, foods, batteries, ferrites, fire retardants and first aid tapes. It occurs naturally as the mineral zincite but most zinc oxide is produced synthetically [8].

1.4.3 Mode of action

There are several hypotheses to explain the antibacterial activity of copper and zinc and a number of factors contributing to contact killing have been identified. The first hypothesis (i) describes copper influx into the cell which causes cell damage. But these surface-released copper ions are not the sole determinant of the process. Another factor that influences cell survival is (ii) oxidative stress. Copper ions induce the generation of reactive oxygen species, which cause further cell damage. The two main factors are the (iii) cell membrane ruptures and the (iv) DNA (Deoxyribonucleic acid) fragmentation, due to presence of copper [9].

Another mechanism possibly explaining the antibacterial properties of zinc oxide nanoparticles (NP) against Escherichia coli is that they changes the cell membrane components including lipids and proteins without significant morphological changes. ZnO NP thus can distort bacterial cell membrane, leading to loss of intracellular components and ultimately the death of cells [10].

1.5 Atmospheric pressure chemical vapour deposition

To produce the thin films with active agents for this study, atmospheric pressure chemical vapour deposition (APCVD) was used. In this section, the current state of the art in plasma deposition using atmospheric pressure plasmas will be discussed.

APCVD is a chemical vapour deposition (CVD) process carried out at atmospheric pressure. In a typical CVD process the substrate is exposed to one or more volatile precursors which react and decompose on the substrate surface to grow thin films. These films can be applied to any kind of substrate, for example steel, glass or highly temperature sensitive materials such as plastics or textiles. In the following, the most important approaches to synthesise films by APCVD are summarised [11].

- Silicon oxide films are of great industrial interest, because of valuable chemical, thermal and optical properties. They are used as a permeation barrier to gas diffusion, as photovoltaic solar cells, as corrosion protection layers and in aeronautical and automotive engineering. They have a good wettability as well, when covered by silanol groups.

- Another inorganic film is titanium oxide. The major application fields of TiO_2 are photocatalysts, chemical sensors, solar cells and dielectric materials. The application potential of these films ranges from self-cleaning, antibacterial to superhydrophilic surfaces.

- Silicon nitride films have been deposited as well. They are optically transparent and present excellent barrier properties. Silicon nitride films are also used for the fabrication of electronic components.

- For layers resistant to electron beams, membranes for gas separation, humidity sensors and optical components, organic films made out of acrylates were used. Due to their good adhesion properties they are often used as a starting point for post deposition of other materials.

- Nowadays, nanotube forests or diamond-like carbon can also be deposited by atmospheric plasma.

- It is possible to combine two precursors; moreover it is possible to combine two precursors in different phases. An example for the latter are dispersed solid nanoparticles in a hexamethyldisiloxane (HMDSO) solution, sprayed in an aerosol form into the gas flow.

The advantages of APCVD are high deposition rates (up to 24 ml/min) and a low consumption of the precursors. Moreover, almost all materials and material assemblies may be deposited, and the process itself acquires lower costs of investment, as there is no need of expensive vacuum technology. On the other hand, toxic reaction products such as nitrogen oxide or ozone are formed during the deposition process. These toxic gases have to be evacuated by an efficient extraction. Another disadvantage is the heat generation during the process and its transport to the coated part due to small distance between the plasma source and the substrate. The quality of the film is strongly dependent on experimental parameters. The main parameters to be controlled are the geometry, the nature of the plasma gas and the state of the precursor. There is still a big field of research, understanding the complex mechanisms that take place at atmospheric pressure. Understanding these phenomena will help to develop technologies as robust as the standard PVD (physical vapour deposition) techniques. Presently, films with a high purity can only be obtained with vacuum based technologies.

2 Thin film deposition

The experimental setup of the deposition system used in this work is schematically shown in Fig. 1. The plasma burner in the facedown arrangement is mounted on a base frame. The substrates are located at a distance of 10 mm below the plasma burner. All samples can be moved on an x-y-positioning stage with a gearless drive [12]. The grid spacing of the film lines was 3 mm by meandering the sample below the burner.
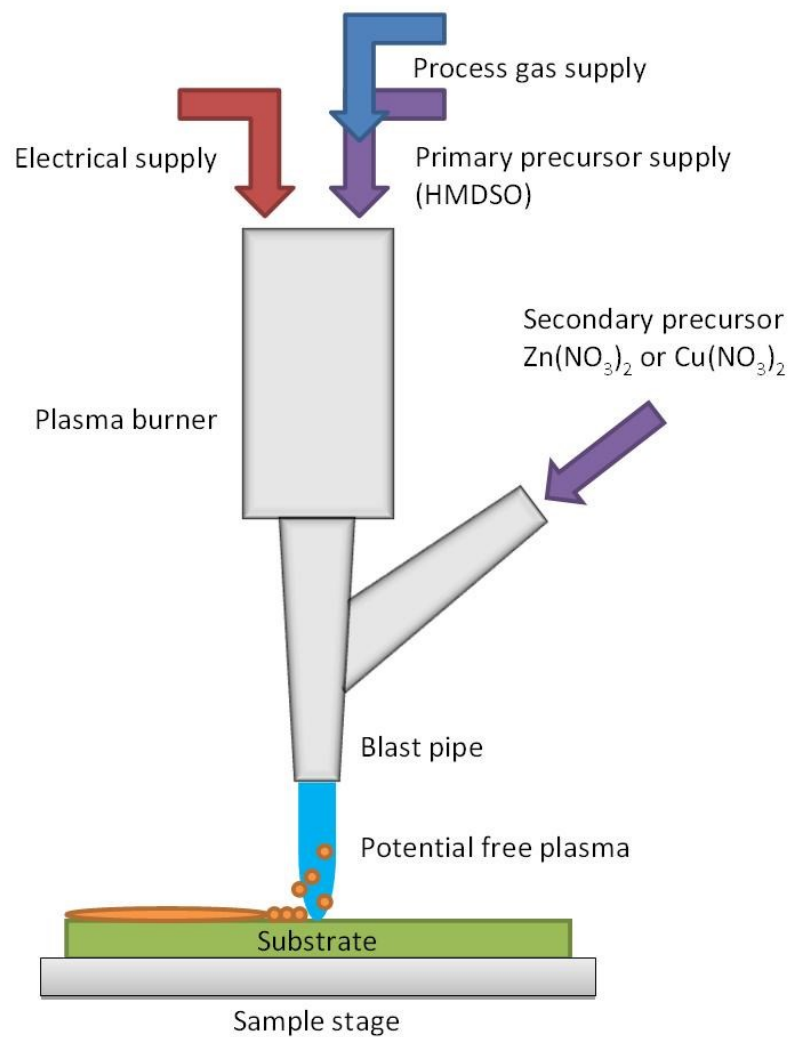

Figure 1: *Scheme of the used APCVD system*

As plasma source, a plasma burner of type BLASTER MEF (TIGRES, Rellingen, Germany) was used in combination with a modified plasma blast pipe, which enabled to feed additives into the plasma. Doing so, copper nitrate $Cu(NO_3)_2$ and zinc nitrate $Zn(NO_3)_2$ were used as secondary precursors.

The source was driven by a low-frequency pulsed direct current (DC) power supply. The plasma burner generated an electrically potential-free air-plasma between an inner stick electrode and an outer blast pipe. The plasma was blown out of the blast pipe by a gas with 6 bar pressure using compressed air. Beside the pressure of the gas, the length of the plasma jet was controlled by the applied power, which was fixed at 400 W. An extra cooling of the electrodes or the substrates was not necessary [13].

As a primary precursor, hexamethyldisiloxane (HMDSO) was used. The precursor was evaporated into a separate air gas flow. As a precursor supply the STS 03 CH (Sura Instruments GmbH, Jena, Germany) was used. The precursor chemically reacts in the plasma of the pipe resulting in SiO_X film deposition on the substrate. The film thickness was controlled by a defined number of repetitive coating runs. Together with the gaseous HMDSO, the $Zn(NO_3)_2$ or the $Cu(NO_3)_2$ solution, respectively, were sprayed into the plasma for the generation of zinc or copper particles, which are subsequently incorporated in the growing SiO_X film. The injection of the solution into the plasma was carried out by use of a dosage nozzle, a peristaltic pump and pressurized air as nebulizer gas [14]. An overview about the settings for all the films prepared within this work is listed in Tab. 2.

Table 2: Settings for surface activation and film deposition

			Activation	Deposition
Applied power		[W]	400	400
Velocity of substrate table		[mm/s]	100	100
Number of runs		[-]	1	8
Process gas		[-]	Air	Air
Process pressure	Blast pipe	[bar]	-	6
	Nebulizer gas	[bar]	-	1.5
Flow rate	Air	[l/min]	-	8
	Primary precursor (HMDSO)	[ml/min]	-	3.5
Grid spacing		[mm]	3	3
Gap		[mm]	10	10

The same plasma parameters, without precursor dosage, were used to activate the sample surface before coating. Of course all parameters contained in table 2 are tuneable. For this work, settings of the SiO_X films established in previous studies were applied [13]. As variable parameters only the flow rate of $Zn(NO_3)_2$ or $Cu(NO_3)_2$ solution, which was used as secondary precursor, were applied.

2.1 Secondary precursor

The solutions of zinc nitrate and copper nitrate served as sprayable additives to generate an antibacterial effect of the film. A solution with correspondingly zinc nitrate or copper nitrate in a 1:1 (v/v) mixture of isopropanol and water was prepared. The settings for the secondary precursor are listed in Tab. 3.

Table 3: Settings of the secondary precursor

Secondary precursor		$Zn(NO_3)_2$			$Cu(NO_3)_2$		
Concentration	[w%]	5			2.5		
Isopropanol:Water	[-]	1:1			1:1		
Solution flow rate	[ml/min]	0.025	0.05	0.1	0.0125	0.025	0.05

The concentration of the Cu(NO3)2 nitrate was reduced by a half compared to Zn(NO3)2, because the copper particles have shown a stronger impact on bacteria and cells. To show the influence of different quantities of copper and zinc particles on the film, three different flow rates were applied.

2.2 Substrates

Implants are typically made of titanium alloyed with aluminium and vanadium (TiAl6V4) according to DIN ISO 5832-3. Medical instruments are made of stainless steel 1.4441 (X2 CrNiMo 18 15 3) according to DIN ISO 5832-1. For the deposition process, round disks made of both materials with diameters of 15 mm and 3 mm in height were used (Königsee Implantate, Aschau, Germany). The surface of these substrates was deburred, polished and glass bead blasted. Before deposition the substrates were cleaned with acetone and isopropanol 1:1 in an ultrasonic bath. The surface roughness R_a of the bare substrates ranged typically between 300 and 600 nm. For characterization of selected film features, silicon wafers were coated.

3 Characterization and analysing methods

"God made the bulk; surfaces were invented by the devil." This note from Wolfgang Ernst Pauli makes clear that the investigation of the surface is exceptionally important and difficult. In this work, special attention was paid to microstructural characterization of the films as well as to wear resistance, cytotoxicity and antibacterial effects.

3.1 Characterization of the film

To understand their functional properties, it is important to analyse the surface of the films as well as their microstructure and chemical composition. In the following paragraphs, some selected analytical methods for imaging the sample surface, for determining chemical composition of the films and for measuring the film roughness are described more in detail.

3.1.1 Scanning electron microscopy

The most useful surface imaging technique is scanning electron microscopy (SEM). The images of a sample surface were obtained by scanning it with a focused electron beam in high vacuum. The interaction of electrons with the sample surface results in secondary electrons, characteristic X-rays, backscattered electrons and Auger electrons, which are either used for the sample imaging or characterization of its elemental composition. According to the required imaging mode, the produced signals were detected with respective detectors.

A common imaging mode for topography contrast is the detection of secondary electrons. The brightness of the signal depends on the number of secondary electrons reaching the detector. Thus, steep surfaces and edges tend to be brighter than flat surfaces, which results in images with a well defined three dimensional appearance [15]. In this mode of imaging by using sensitive detectors, an image resolution less than 0.5 nm can be reached.

3.1.2 Energy dispersive X-ray spectroscopy

Energy dispersive X-ray spectroscopy (EDX) is a common analytical technique to determine the qualitative and quantitative material composition. EDX mapping provides in addition to the conventional SEM image a picture of the element distribution of a surface. By this technique, the characteristic X-rays generated in the irradiated area of the specimen are analysed. To stimulate the emission of characteristic X-rays, the electron beam within the SEM is focused on the sample surface being studied. The incident beam excites an electron

in an inner shell of a sample. An electron hole is created by ejecting the electron from the shell, which is filled by an electron from an outer, high-energy shell. The energy difference between the higher and the lower energy shell results in a release of a characteristic X-ray. The intensity and energy of the X-rays emitted from a specimen is subsequently analysed by an energy dispersive spectrometer giving a fingerprint of the elemental composition of the measured area of the sample [16]. The information depth for the method is about 1 µm, which corresponds to the irradiated volume of the sample.

3.1.3 X-ray photoelectron spectroscopy

X-ray photoelectron spectroscopy (XPS) is a surface analysis technique that measures elemental compositions, chemical and electronic state of the elements that exist within a material. In ultra-high vacuum the specimen is exposed to an X-ray beam, while simultaneously measuring the kinetic energy and number of electrons that escape from the material. XPS cannot detect hydrogen and helium because the binding energy is so small compared to the excitation energy of X-ray photon and hence the absorption efficiency is very small. Detection limits for most of the elements are in the parts per thousand ranges [17]. In this work, an XPS system (Theta Probe, Thermo VG Scientific, East Grinstead, Great Britain) was used providing an information depth in the range of 1 to 10 nm.

3.1.4 Atomic force microscopy

Atomic force microscopy (AFM) is a tool for imaging, measuring and manipulation of the specimen surfaces. The information is gathered by scanning the surface using a cantilever with a sharp tip. To detect the deflection of the cantilever, a fibre optic interferometer is used. Operation of an AFM can be done in contact, non-contact and tapping mode.

A common method is the non-contact mode. In this mode the tip of the cantilever does not contact the sample surface. The tip is oscillated via excitation of the cantilever-piezo. The distance between tip and sample is controlled by the amplitude of the cantilever. Measuring the tip to sample distance at each point allows the scanning software to construct a topographic image of the sample surface. The method allows less wear on the tips, since no load force or friction load appears [18].

By using the AFM within this study in the non contact mode (SIS UltraOBJECTIVE, SIS GmbH, Herzogenrath, Germany), an image with a maximum height of 2 µm and a maximum scanning area of 20 x 20 µm can be recorded [19].

3.2 Washability test

To probe the resistance of the films against abrasive wear and consequentially the corresponding residual antiseptic effect of the films, a washability test was performed. Nylon brushes (Elcometer, Aalen, Germany) and a holder of stainless steel with standardized mass were both conform to the ASTM D2486, describing a test method for determination of scrub resistance. Distilled water was used in a washability tester (Simex, Haan, Germany). For this test, the samples were fixed with polyamide film tape on a glass plate. The number of washing cycles was varied from 1000 to 10 000 cycles.

3.3. Cytotoxic test

The MC 3T3-E1 mouse calvaria derived cell line has been used to study the possible cytotoxic effect of the film. The FDA/GelRed live/dead staining test is a two colour assay to determine living and dead cells [20]. The green fluorescent cyto dye (FDA) is used to stain the live cells and the red fluorescent cyto dye (GelRed) is used to stain dead cells.

3.3.1 Mouse cells

The osteoplastic cell line MC 3T3-E1 (DSMZ, Braunschweig, Germany), as it is pictured in Fig. 2, has been established from mouse calvaria [21]. The capability of these cells to adhere not only on bones but on implants and form calcified bone tissue in vitro is important for an efficient wound healing process. The possible cytotoxic effect of the film, which is doped with Zn or Cu, has to be avoided. The cells have an adherent growth mode and their morphology is fibroblast-like. The cells are typically spread homogenously in all directions, with a size of 100 µm.
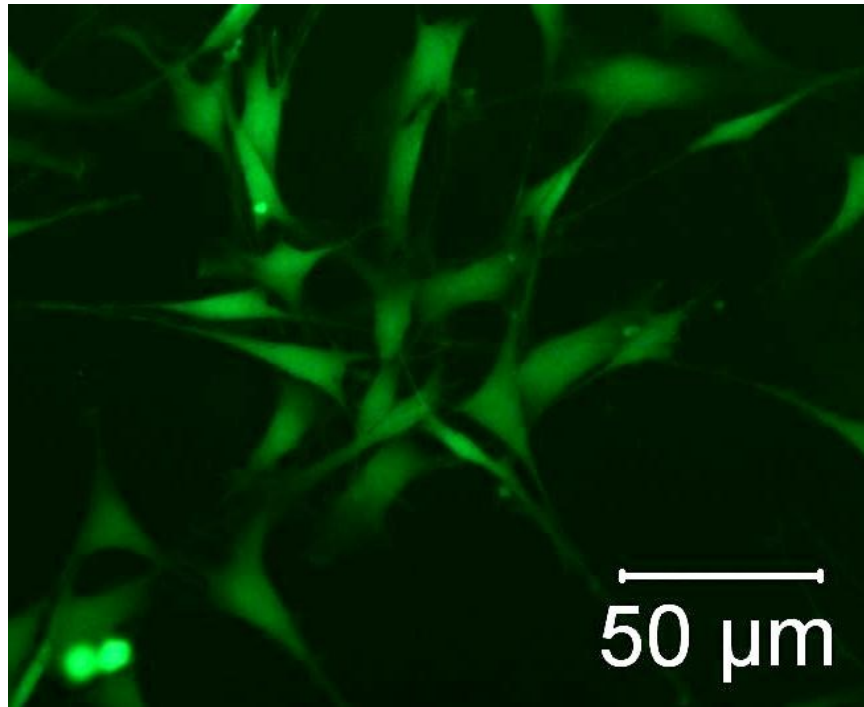
Figure 2: *Fluorescence micrograph of a cluster of MC 3T3-E1*

3.3.2 Cell cultivation

In cell culture, passaging is the process of sub-culturing cells in order to produce a large number of cells from pre-existing ones [22]. Passaging involves splitting the cells and transferring into a new vessel.

Adherent cells, like MC 3T3-E1, are grown in culture flasks with culture media at 37 °C and 5 % CO_2. As culture media 80 – 90 % Alpha medium supplemented with nuceleosides (Biochrom, Berlin, Germany), 10 % calf serum and 2 mmol/l L-alanyl-L-glutamine as a substitutes for L-glutamine, is used. After one week the confluency is reached and passing is required. Thus, the media is removed and the cells are washed with phosphate buffered saline (PBS). Then trypsin EDTA (Ethylene diaminetetraacetic acid) is added to make cells detach from the bottom of the flask. To stop the reaction the cells are resuspended in PBS, which acts as trypsin inhibitor. An appropriate number of cells in suspension is then transferred into a new flask, fresh culture media is added and the flask is incubated for the next growth phase [22]. After one day the cells are ready to use for the life/dead assay.

3.3.3 Life/dead assay

The live/dead staining is based on the fact that living cells show a green fluorescent cytoplasm while dead cells show a red fluorescent one [20]. The added dye fluoreszeindiacetat (FDA) converts enzymatically to the green fluorescent dye fluorescin,

which causes the green fluorescent colour of the vital cells. The necrotic or dead cells have a more permeable cell membrane than living cells. GelRed enters into the cell and attaches to the nucleic acids which cause the red fluorescent colour.

Prior the test, the substrates were sterilized for half an hour in 70 % ethanol, after that the substrates were washed with phosphate buffered saline (PBS). For the test, the cells were brought into direct contact with the film in a density of about 12 500 cells/cm^2. The cells were cultured inside a cell incubator (BINDER GmbH, Tuttlingen, Germany) under 37 °C and 5 % CO_2 atmosphere. After one, three and seven days of incubation, the live/dead staining test was performed. For this purpose, a 50 µl combination colour solution, which contains FDA, GelRed and PBS, was applied. Pictures of the cell colouration were taken, the cell number was counted and the percentage of dead cells evaluated using a fluorescence microscope (Axiotech, Zeiss, Jena, Germany).

3.4 Antibacterial test

The antibacterial effect of the film was probed using an Escherichia coli (E. coli) strain (see section 3.4.1). The BacTiter-Glo (BTG) microbial cell assay (Promega, Madison, Wi, USA) was used to detect bacterial injury on the basis of the intracellular adenosine triphosphate (ATP) content of the cells [23].

3.4.1 Escherichia Coli

The bacteria strain used for this study was E. coli (HB 101-strain), as it is shown in Fig. 3. Almost all strains of E. coli are harmless and actually are an important part of a healthy human intestinal tract. Some kinds of E. coli are pathogenic, they cause diarrhea, urinary tract infections, respiratory illness and pneumonia [24].

Figure 3: Low-temperature SEM micrograph of a cluster of E. coli bacteria [25]

The bacteria belongs to the family of Enterobacteriaceae, it is non-sporulating, facultative anaerobic and gram-negative. E. coli are typically rod-shaped with a length of 2 µm and 0.5 µm in diameter. The bacteria can live on a wide variety of substrates [26].

3.4.2 Cultivation of bacteria

The cultivation of bacteria starts on the day prior the evaluation day. As a sterile culture medium, soya bean casein digest medium (SIFIN, Berlin, Germany) was used. The culture medium (25 µm) were inoculated with E. coli (100 µm) and cultivated in an incubator at 37°C for 18 hours. The multiplication of the bacteria is exponentially growing.

Subsequently, 10 ml of the medium was refreshed with 10 ml of fresh, new culture medium. This working suspension was newly cultured at 37°C for 2 hours. In such a way standard terms are created.

Further, the bacteria were centrifuged at 2000 rpm for 15 minutes and immediately resuspended in physiological saline 0.9 (w/v). By removing the culture medium and replacing with physical saline, stable growth conditions were established and the osmotic balance can be remained. For this study around 200 000 cells were engaged.

3.4.3 BacTiter-GloTM (BTG) assay

The BacTiter Glo^{TM} microbial cell viability assay (Promega, Madison, WI, USA) is a homogeneous method for determining the number of viable microbial cells in the culture based on quantization of the ATP present. ATP is an indicator of metabolically active cells.

For the test, the E. coli were brought in direct contact with the film and the coated samples covered by the E. coli suspension were transferred to a 24 well cell culture plate (CELLSTAR, Greiner Bio-One, Frickenhausen, Germany). Each sample was immersed in 0.5 ml of the diluted E. coli working suspension for 3 hours. After this incubation step, volume parts of 50 µl were transferred into a white non-transparent 96 well plate. Aliquots taken from uncoated reference samples were also included. To get a representative value, at least three replicates were used. Finally, 50 µl BTG reagents were added to each sample and mixed at a mixmate microplate shaker (Eppendorf, Hamburg, Germany) for 5 min at 850 rpm. Developed luminescence signals were measured thereafter in a microplate reader enabling luminescence detection (Genios Pro, Tecan, Crailsheim, Germany) using an integration time of 400 ms. An antibacterial effect was detected if the BacTiter-Glo test showed a decrease of luminescence in comparison to the not affected control [13].

Bibliography

[1]   Council directive 93/42/EEC concerning medical devices, EUR-Lex, June 1993

[2]   Wikipedia, Wound, http://en.wikipedia.org/wiki/Wound, July 2013

[3]   R. F. Diegelmann, M. C. Evans, Wound healing: An overview of acute, fibrotic and delayed healing, Frontiers of Bioscience 9 (2004) 283-289

[4]   Wikipedia, Implant (medicine), http://en.wikipedia.org/wiki/Implant_%28medicine%29, July 2013

[5]   G. E. Morfill, J. L. Zimmermann, Plasma Health Care – Old problems, new solutions, Contributions to Plasma Physics 52, 7 (2012) 655-663

[6]   Wikipedia, Copper, http://en.wikipedia.org/wiki/Copper, July 2013

[7]   Wikipedia, Zinc, http://en.wikipedia.org/wiki/Zinc, July 2013

[8]   Wikipedia, Zinc oxide, http://en.wikipedia.org/wiki/Zinc_oxide, July 2013

[9]   G. Grass, Ch. Rensing, M. Solioz, Metallic copper as an antimicrobial surface, Applied and environmental microbiology 77, 5 (2011) 1541-1547

[10] Y. Liu, L. He, A. Mustapha, H. Li, Z.Q. Hu, M. Lin, Antibacterial activities of zinc oxide nanoparticles against Escherichia coli O157:H7, Journal of Applied Microbiology, 107 (2009) 1193-1201

[11] D. Merche, N. Vandencasteele, F. Reniers, Atmospheric plasmas for thin film deposition: A critical review, Thin Solid Films 520 (2012) 4219-4236

[12] A. Pfuch, K. Horn, R. Mix, M. Ramm, A.Heft, A. Schimanski, Direct and remote plasma assisted CVD at atmospheric pressure for the preparation of oxide thin films, in R. Suchentrunk (ed.), 2010 Jahrbuch Oberflächentechnik Band 66, (2010) 114-115

[13] R. Zimmermann, A. Pfuch, K. Horn, J. Weisser, A. Heft, M. Röder, R. Linke, M. Schnabelrauch, A. Schimanski, An approach to create silver containing antibacterial coatings by use of atmospheric pressure plasma chemical vapour deposition (APCVD) and combustion chemical vapour deposition (CCVD) in an economic way, Plasma Processes and Polymers 8 (2011) 295-304

[14] O. Beier, A. Pfuch, K. Horn, J. Weisser, M. Schnabelrauch, A. Schimanski, Low temperature deposition of antibacterially active silicon oxide layers containing silver nanoparticles, prepared by atmospheric pressure plasma chemical vapour deposition, Plasma Processes and Polymers 10 (2012) 77-87

[15] Wikipedia, Scanning electron microscope, http://en.wikipedia.org/wiki/Scanning_electron_microscope, August 2013-08-29

[16] Wikipedia, Energy-dispersive X-ray spectroscopy, http://en.wikipedia.org/wiki/Energy-dispersive_X-ray_spectroscopy, August 2013

[17] Wikipedia, X-ray photoelectron spectroscopy, http://en.wikipedia.org/wiki/X-ray_photoelectron_spectroscopy, August 2013

[18] Bruker Nano, Nanos ScanPanel User Guide, Version 1.2, May 2009

[19] Universität des Saarlandes, SIS UltraObjective, http://www.uni-saarland.de/fak7/hartmann/de/research/instrumentation/SIS.htm, August 2013

[20] Life technologies, Live/dead cell viability assay, http://www.lifetechnologies.com/at/en/home/brands/molecular-probes/key-molecular-probes-products/live-dead-viability-brand-page.html, October 2013

[21] DSMZ, Deutsche Sammlung von Mikroorganismen und Zellkulturen, http://www.dsmz.de/, October 2013

[22] Carl Roth, Cell passage and use of trypsin, http://www.carlroth.com/website/fr-fr/pdf/Zellpassage_Trypsin_E.pdf, August 2013

[23] Promega, Cell viability assays, http://www.promega.co.uk/products/cell-health-and-metabolism/cell-viability-assays/, September 2013

[24] Centers for Disease Control and Prevention, General information Escherichia coli, http://www.cdc.gov/ecoli/general/index.html, August 2013

[25] Wikipedia, E coli at 10000x, original http://en.wikipedia.org/wiki/File:E_coli_at_10000x,_original.jpg, August 2013

[26] Wikipedia, Escherichia coli, http://en.wikipedia.org/wiki/Escherichia_coli, August 2013

[27] S. Spange, Antibakterielle Beschichtungen auf Textil (Wundauflagen), Ernst-Abbe-Fachhochschule Jena, Diploma Thesis, October 2012

[28] L. Friedrich, Einfluss unterschiedlicher Silber- und Kupfer Konzentrationen in der SiO_X Beschichtung von Titan-Aluminium6-Vanadium4-Calciumphosphat auf die bakterizide und zytotoxische Wirkung der Oberfläche, Ernst-Abbe-Fachhochschule Jena, Bachelor Thesis, August 2012

4 Manuscript

E. Jäger, J. Schmidt, A. Pfuch, S. Spange, O. Beier, R. Daniel, O. Jantschner, C. Mitterer

Antibacterial silicon oxide films doped with zinc and copper for medical applications grown by atmospheric pressure plasma chemical vapour deposition

E. Jäger, R. Daniel, O. Jantschner, C. Mitterer,

Department for Physical Metallurgy and Materials Testing, Montanuniversität Leoben, Roseggerstrasse 12, 8700 Leoben, Austria

J. Schmidt, A. Pfuch, S. Spange, O. Beier

INNOVENT e.V. Technology Development Jena, Pruessingstrasse 27B, 07745 Jena, Germany

Corresponding author: E. Jäger

E-mail address: elisabeth.jaeger@stud.unileoben.ac.at

Tel.: +43 699 11042754

Fax: +43 3842 402 4202

Abstract

The antibacterial effect against Escherichia coli and the cytotoxic activities against mouse calvaria derived cell line (MC 3T3-E1) was studied for copper- and zinc-doped silicon oxide films grown by atmospheric pressure chemical vapour deposition. The antibacterial effect of the films is related to the formation of copper and zinc oxide particles, homogeneously distributed on the film surface. The bacteria are killed already within the first three hours after exposure to the antiseptic particles. The higher release of copper or zinc in the first days inhibited also cell growth, which is less pronounced in the initial stage of the test. The obtained results indicate that the films have a high potential to be used as effective antibacterial films in medical applications.

1 Introduction

Implants like surgical nails, screws and plates are commonly used to fixate the fractured bone to ensure a successful healing process. If any part of the healing sequence is altered by microorganisms [1], the healing process will be extended dramatically. One possible solution to protect the patient from infection, sepsis and putrefaction is to coat the implant with films containing antiseptic elements like silver (Ag), zinc (Zn) or copper (Cu) [2]. Atmospheric pressure chemical vapour deposition (APCVD), combustion chemical vapour deposition [3] and physical vapour deposition [4,5] are common methods to deposit such antibacterial coatings. The aim of this study was to produce bio-compatible silicon oxide (SiO_x) films doped with the antiseptic elements Zn and Cu, with a significant antimicrobial effect against Escherichia coli (E. coli) and a sufficient growth and vitality of mouse cells of type MC 3T3-E1. The microstructure, chemical composition, antibacterial effect and cell growth were studied, as well as the influence of sterilisation and washing procedures, to identify and improve the antibacterial effect through optimisation of film composition.

2 Materials and Methods

2.1 Substrates

Aluminium and vanadium alloyed titanium (TiAl6V4) (DIN ISO 5832-3) and stainless steel 1.4441 (X2 CrNiMo 18 15 3) (DIN ISO 5832-1) round disks of 15 mm in diameter and 3 mm in height (Königsee Implantate) were used for deposition of $Cu-SiO_x$ and $Zn-SiO_x$ films by APCVD. For scanning electron microscopy (SEM), energy dispersive X-ray spectroscopy (EDX), atomic force microscopy (AFM) and X-ray photoelectron spectroscopy (XPS), silicon wafers (10 x 20 mm) were coated.

2.2 Thin film deposition

The APCVD technique combining a typical CVD process with a plasma discharge at atmospheric pressure was used to deposit the films. In a typical CVD process, the substrates are exposed to volatile precursors, which react and decompose on the substrate. As primary precursor, hexamethyldisiloxane (HMDSO) was used to create the SiO_x matrix. As secondary precursors, solutions with Cu nitrate $Cu(NO_3)_2$ or Zn nitrate $Zn(NO_3)_2$ in a 1:1 mixture of isopropanol and water, were used. The variable parameters to adjust the Cu and Zn content were the flow rates of the $Cu(NO_3)_2$ and $Zn(NO_3)_2$ solutions, respectively. The settings for the

secondary precursors are listed in Tab. 1. The DC (direct current) pulsed plasma was subsequently ignited between two cylindrical electrodes, an inner stick metallic electrode and the actual plasma nozzle as grounded outer electrode. The substrates were located at a distance of 10 mm below the plasma burner. The grid spacing of the film lines was 3 mm by meandering the sample below the burner. To achieve a film thickness of 100 nm, 8 runs during the deposition process were done. As plasma source, a plasma burner BLASTER MEF (TIGRES) was used in combination with a modified plasma blast pipe, which enabled to feed additives into the plasma. The plasma jet was accelerated using compressed air at a pressure of 6 bar. The length of the plasma jet was controlled by the applied power set to 400 W. Further details on the APCVD process are reported in previous papers [3,6,7].

Table 1: *Settings of the secondary precursors*

Secondary precursor		$Zn(NO_3)_2$			$Cu(NO_3)_2$		
Concentration	[wt %]	5			2.5		
Isopropanol:Water	[-]	1:1			1:1		
Flow rate	[µl/min]	25	50	100	12.5	25	50

2.3 Characterisation of the films

For imaging the film surface, a SEM (SUPRA 55 VP, Carl Zeiss) was used. The film thickness was measured using a stylus contact profilometer (Dektak3 ST). The chemical composition of the films was determined by EDX (Si(Li) detector, Röntec) and XPS (Theta Probe, Thermo VG Scientific). The oxidation states of Zn, Cu and Si were identified with an X-ray excitation energy of 1468.68 eV (Al-Kα-line). The 2p core levels were used for the determination of the metal oxides. No thermal treatment or sputter cleaning of the surface was included prior to the measurements. As energy calibration, the binding energy of the C1s level (285 eV) taken from the carbon surface contamination was used. The average film roughness R_a was measured and imaged by an AFM (SIS UltraOBJECTIVE, SIS) in the non-contact mode. To probe the resistance of the films against abrasive wear and consequentially the corresponding residual antiseptic effect of the films, a washability test (Simex) in distilled water was performed. Nylon brushes (Elcometer) and a stainless steel holder were both conform to the ASTM D2486 standard. The number of washing cycles was varied from 1000 to 10 000.

The FDA/GelRed live/dead staining test was used to study the cytotoxic effect of the films on MC 3T3-E1 mouse cells. For the test, the cells were brought into direct contact with the film

surface in a density of about 12 500 cells/cm^2. After one, three and seven days of incubation, the live/dead staining test was performed. The cell colouration micrographs were taken using an Axiotech fluorescence microscope (Carl Zeiss).

The antibacterial effect of the films was probed using an Escherichia coli (E. coli) strain. The BacTiter-Glo (BTG) microbial cell assay (Promega) was used to detect bacterial injury on the basis of the intracellular adenosine triphosphate (ATP) content of the cells. For the test, the E. coli were brought in direct contact with the film surface. Each sample was immersed in 0.5 ml of the diluted E. coli working suspension for 3 hours. The developed luminescence signals were recorded in a microplate reader (Genios Pro, Tecan) enabling luminescence detection using an integration time of 400 ms. An antibacterial effect was detected if the BTG test showed a decrease of luminescence in comparison to the not affected control.

Sterilisation tests were performed under hospital cleaning and sterilisation conditions (Thüringen-Kliniken "Georgius Agricola") to test the antibacterial effect of the films after such treatment. The cleaning step over 50 min was realized by a cleaning, disinfection and drying machine WD380 (Belimed), with a washing temperature of 93 °C and a drying temperature of 110 °C. The followed sterilisation step of 5 min was performed by a steam-steriliser Selectomat (MMM) in a temperature range of 134 to 137 °C and a pressure between 3034 and 3320 mbar. Subsequently, the BTG test was performed on the film surface.

3 Results

3.1 Morphology

All films having a constant thickness of 100 nm were optically transparent and well adherent to the substrates. The SiO$_x$ films doped with Zn or Cu exhibit a surface roughness R_a in the range of 400 to 1100 nm. The higher values are related to the increased formation of CuO$_x$ and ZnO$_x$ particles at higher secondary precursor flow rates (see Fig. 1a), which is a typical feature of the APCVD process [7]. By changing the flow rate of the secondary precursor from 12.5 to 100 µl/min, the particle size apparently changes from 0.5 to 1.2 µm for the doped coatings. In contrast, SiO$_x$ particles of only 200 nm in size formed during deposition of the SiO$_x$ films.

3.2 Chemical composition

The EDX map of the Zn-SiO$_x$ film surface depicted in Fig. 1b shows the ZnO$_x$ particles formed during deposition at a flow rate of 100 µl/min. Besides these particles, a uniform distribution

with a lower Zn concentration was also detected on the film surface. The formation of CuO_x particles on the surface of the $Cu-SiO_x$ films with similar distribution indicates the same growth mechanism of the particles as in the case of the $Zn-SiO_x$ films.
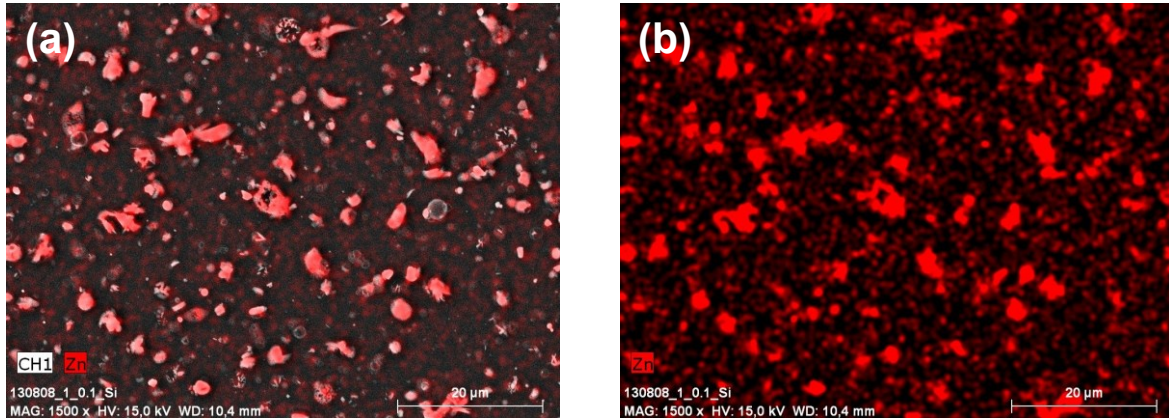

Figure 1: (a) SEM surface morphology and (b) the corresponding EDX mapping of Zn for a Zn-SiOx film deposited on a silicon wafer with a secondary precursor flow rate of 100 μl/min.

Fig. 2 shows the XPS spectra of the Zn doped SiO_x film grown at the highest flow rate of the secondary precursor of 100 µl/min. Peak fit analysis was used to separate the Si 2p (Fig. 2a), C 1s (Fig. 2b) and O 1s (Fig. 2c) spectra into individual components. The peaks in Fig. 2a located at 103.9 and 102.2 eV correspond to the Si-O and Si-N bonding, respectively, which is in a good agreement with the findings of Wagner et al. [8]. The Si-N bonding originates from the small amount of nitrogen incorporated in the films from fractions of not fully dissipated secondary precursor. The two peak positions in Fig. 2c located at 533.3 and 531.5 eV correspond to the Si-O and Zn-O bonding. The absence of the Si-Si and Zn-Zn bonding indicates full oxidisation of the film (besides the minor nitride fraction mentioned above), which is due to much higher enthalpy of formation of the oxide components with respect to the metallic bonding [8]. The Zn content of the doped films of 2.3 at.% at a secondary precursor flow rate of 100 µl/min decreases with decreasing flow rate, which is reflected by a reduced Zn $2p^{3/2}$ signal.

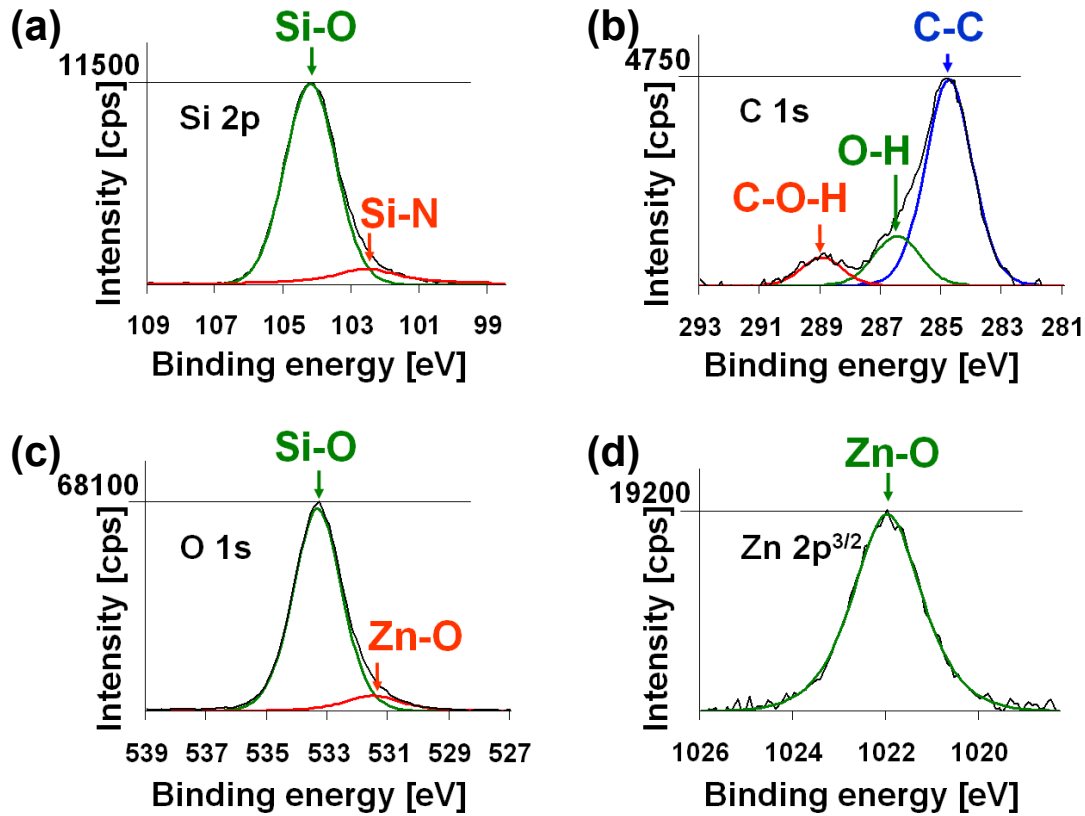**Figure 2:** *XPS spectra of the Zn-SiO$_X$ film grown with the secondary precursor flow rate of 100 µl/min. Note the difference scales in Fig. 2a-d.*

Fig. 3 shows the XPS spectra of the Cu doped SiO$_x$ film grown at the highest secondary precursor flow rate of 50 µl/min. The Si 2p (Fig. 3a), C 1s (Fig. 3b) and O 1s spectra (Fig. 3c) were again separated into their individual components. The peaks in Fig. 3a located at 103.5 and 101.6 eV correspond to the Si-O and Si-N bonding, respectively, which is again in good agreement with the findings of Wagner et al. [8]. Likewise, the Si-N bonding originates from the small amount of nitrogen incorporated in the films from the not fully dissipated secondary precursor. The two peak positions in Fig. 3c located at 533.1 and 530.6 eV correspond to the Si-O and Cu-O bonding. Also here, the absence of the Si-Si and Cu-Cu bonding indicates full oxidisation of the film, which is due to much higher enthalpy of formation of the oxide components with respect to the metallic bonding [8]. This result is in good agreement with the findings of Maroie et al. [9]. The qualitative analysis is similar to the Zn-SiO$_x$ films; however, lower Cu concentrations were obtained. For a secondary precursor flow rate of 50 µl/min, a Cu content of about 0.2 at.% was obtained.
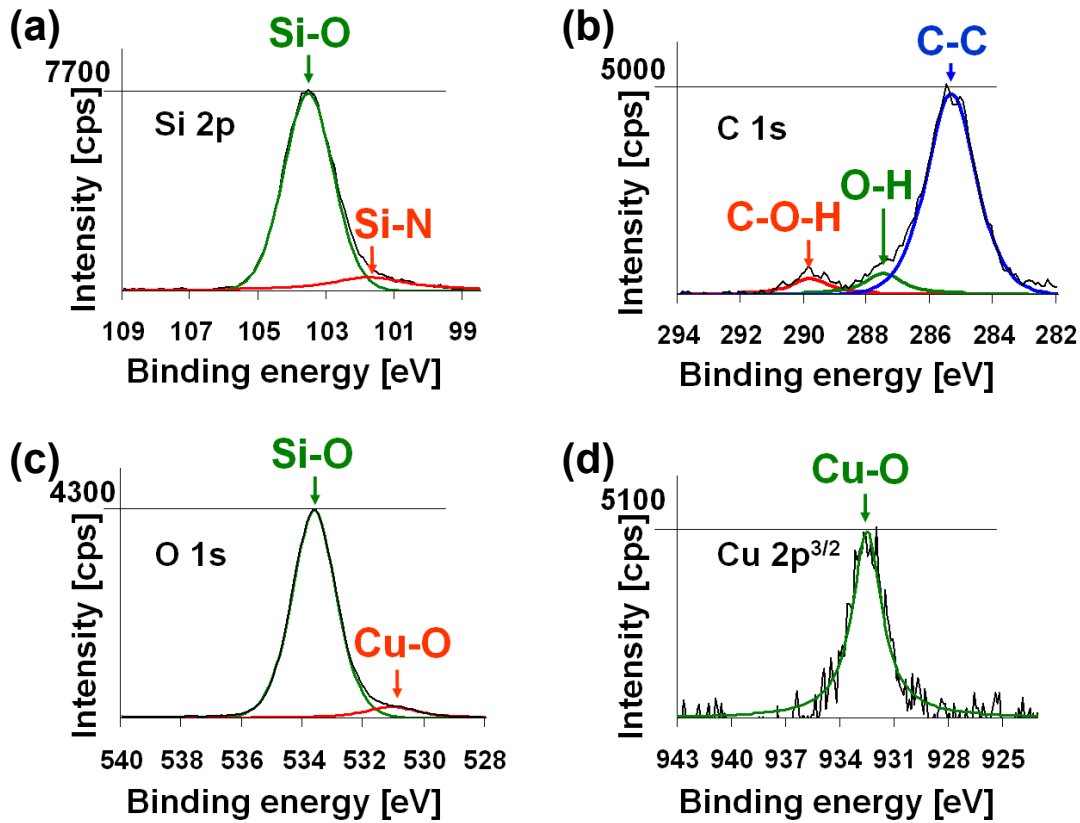
Figure 3: *XPS spectra of the Cu-SiO$_X$ film grown at a secondary precursor flow rate of 50 µl/min. Note the difference scales in Fig. 3a-d.*

3.3 Cytotoxic effect

The development of the number of grown MC 3T3-E1 cells on the surface of the Cu and Zn doped SiO$_x$ films during the live/dead staining test on two replicates (TiAl6V4 and stainless steel substrates) is visualised in Fig. 4 for the films grown at the highest flow rates of the secondary precursors. A loose green fluorescent cell floor (negligible number of dead cells) shows spread cell formation after staining the samples after the one day incubation, regardless of the flow rate (Fig. 4a, d). The uncoated reference samples showed the same loose green fluorescent cell floor, which indicates no cytotoxic effect. The micrographs in Fig. 4b and 4e still indicated no cytotoxic effect, but a certain inhibition in cell growth after three days. A dramatic increase of the cell density on the film surface after 7 days of the test evidences an unhampered cell growth (Fig. 4c, f). The development of the cell growth in the case of SiO$_x$ is similar to the doped films, evidencing that the addition of Cu and Zn does not affect the cytotoxic effect.
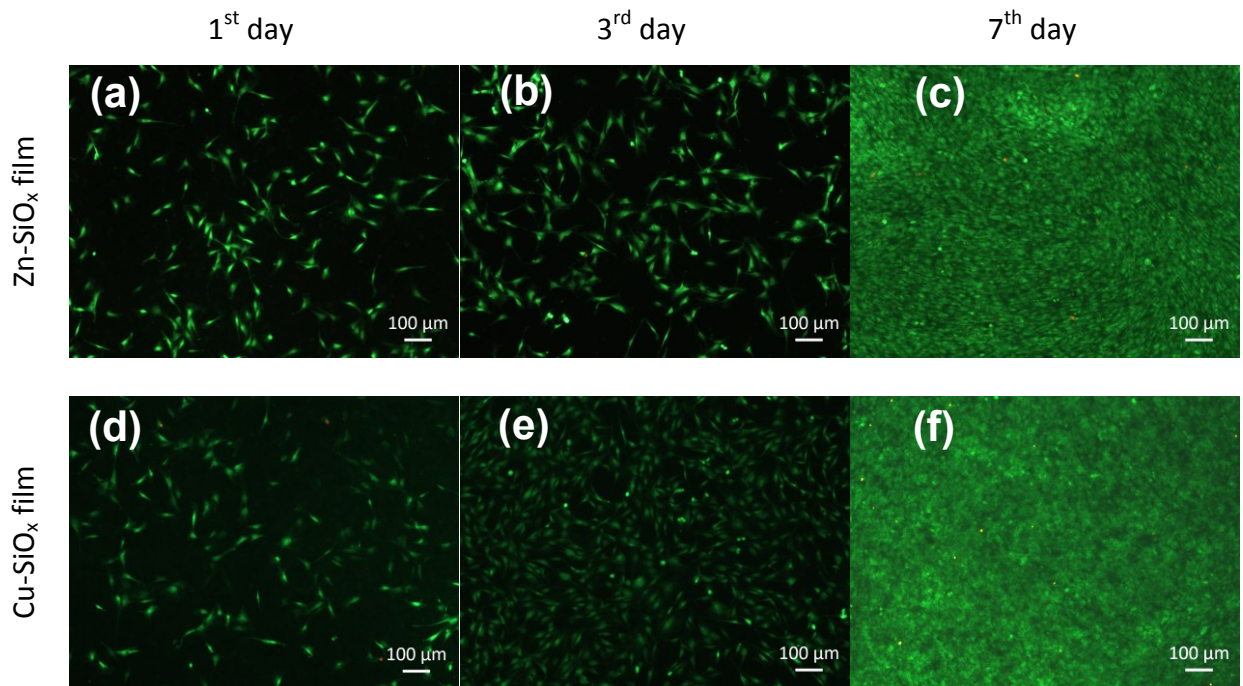
Figure 4: *Live/dead staining images for a Zn-SiO$_x$ film grown at a secondary precursor flow rate of 100 µl/min flow rate **(a-c)**, and for a Cu-SiO$_x$ film grown at 50 µl/min **(d-f)** on the first **(a, d)**, third **(b, e)** and seventh evaluation day **(c, f)**.*

3.4 Antibacterial activity

Fig. 5 shows that the antibacterial activity of the Zn-SiO$_x$ films, expressed by the luminescence of ATP with respect to the uncoated reference sample, for the increasing Zn(NO$_3$)$_2$ flow rate. For these experiments, a secondary precursor concentration of 5 % and three different flow rates, i.e. 25, 50 and 100 µl/min, were used, which correlates with the Zn concentration in the coating. A slight decrease of the luminescence of ATP is visible with increasing Zn(NO$_3$)$_2$ flow rate. The film with the lowest Zn fraction shows a luminescence of ATP of 11 % at the Ti6Al4V substrate and 23 % at the stainless steel substrate. For a detectable antibacterial activity, a secondary precursor flow rate of 25 µl/min was sufficient. It should be noted here that the substrate material did not show a pronounced effect on the antibacterial activity.
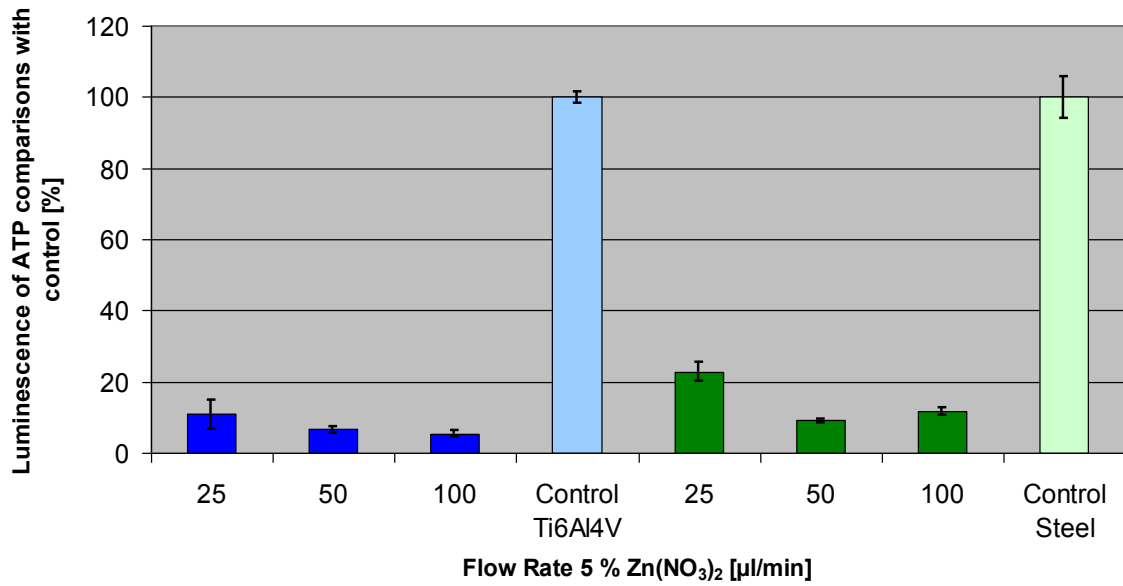
Figure 5: *Influence of the flow rate used for Zn-SiO$_x$ samples coated with a secondary precursor concentration of 5 % Zn(NO$_3$)$_2$ on detectable ATP.*

Compared to the Zn-SiO$_x$ system, the Cu-SiO$_x$ system showed a more pronounced antibacterial effect, irrespective of the film composition and used substrate, even for a reduced Cu(NO$_3$)$_2$ concentration of 2.5 % (Fig. 6). The antibacterial effect is evident for Cu-SiO$_x$ films having a much lower Cu content compared to the Zn content of the Zn-SiO$_x$ films (see section 3.2 and compare Figs. 5 and 6). The luminescence of ATP decreased to 1 %.
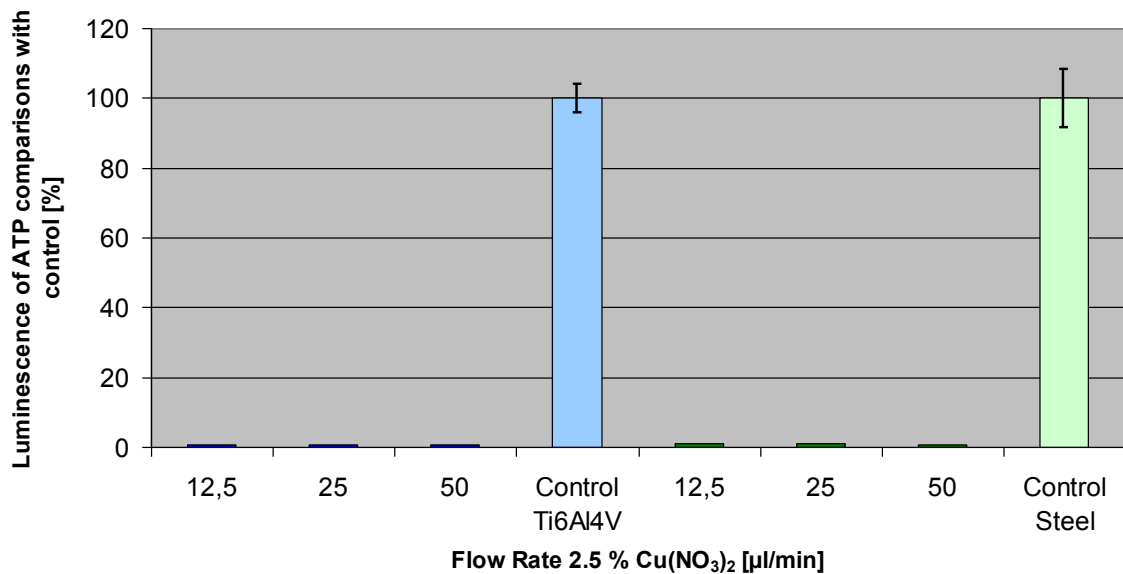

Figure 6: *Influence of the flow rate used for Cu-SiO$_x$ samples coated with a secondary precursor concentration of 2.5 % Cu(NO$_3$)$_2$ on detectable ATP.*

The abrasion of the film surface during the washability test results in a modification of morphology, as shown for the Zn-SiO$_x$ film after 1000 washing cycles in Fig. 7. The sample surface was significantly smoother (R_a = 500 nm) compared to the unstressed reference sample (R_a = 1100 nm). Most of the ZnO$_x$ particles formed on the film surface during the deposition process were scrubbed from the surface, which also changes the composition of the film surface (the highest Zn concentration was detected in the particles, see Fig. 1).
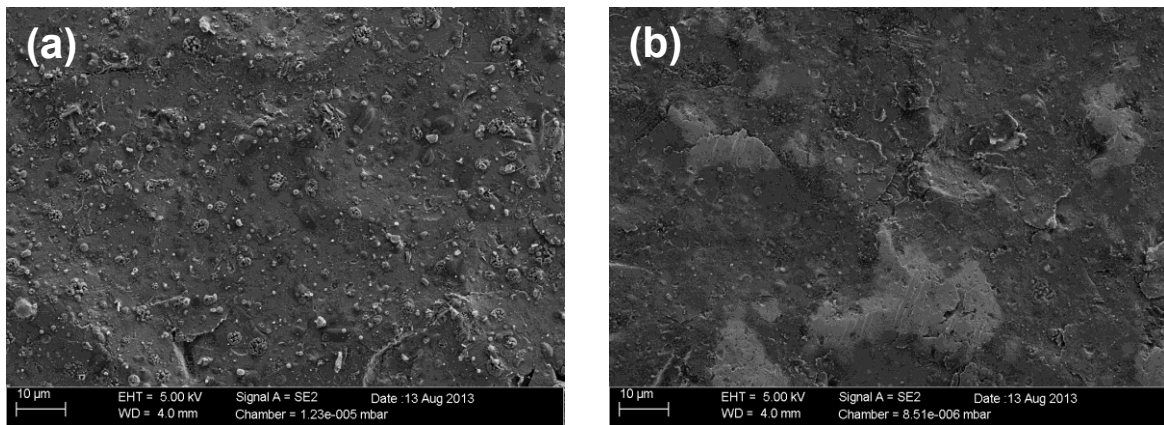

Figure 7: *SEM images of Zn-SiO$_x$ films on stainless steel coated with a secondary precursor concentration of 5 % Zn(NO$_3$)$_2$ and a flow rate of 100 µl/min. (a) as-deposited and (b) after 1000 washing cycles*

This affects the antibacterial ability of the film as shown in Fig. 8. Here, the luminescence of ATP on the surface of the Cu-SiO$_x$ films is given after 1000 washing cycles, which is higher than that of the sample prior to the test (see Fig. 6), predominantly for the film with the lowest Cu fraction. With increasing Cu content in the film, the difference in the antibacterial behaviour decreases. After 10 000 washing cycles, no reliable antibacterial effect was detected, because of the inhomogeneous and partly degraded film.
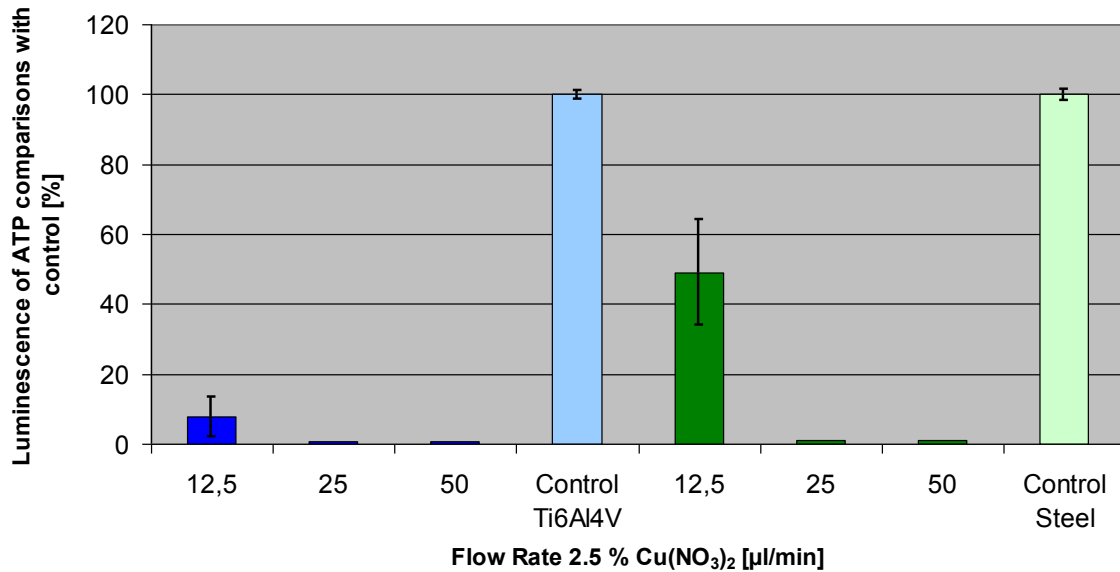
Figure 8: *Influence of the flow rate used for a secondary precursor concentration of 2.5 %*
$Cu(NO_3)_2$ to grow Cu-SiO$_x$ samples on detectable ATP, after 1000 washing cycles.

Fig. 9 shows a strong increase in the luminescence signals after 1000 washing cycles, reaching higher values than prior to the test, except for the coating with the highest Zn fraction (see Fig. 5). With increasing Zn content in the film, the difference in the antibacterial behaviour is increasing. The film with the lowest amount of Zn shows a luminescence of ATP of 80 % on the Ti6Al4V substrate and 59 % on the stainless steel substrate. For the film with the intermediate Zn fraction, a luminescence of ATP of 24 % on both substrates was obtained. After 10 000 washing cycles, the films lost their antibacterial functionality.

During sterilisation, the film surface is exposed to heat, pressure and chemicals like ethanol, which typically affects its antibacterial functionality. The effect of the sterilisation process on the antibacterial behaviour of the Cu-SiO$_x$ film with the Cu content of 0.2 at.% is shown in Fig. 10. The luminescence of the ATP after 15 sterilization cycles shows an increase of 170 % compared to the as-deposited film. After 30 cycles, an increase of about 200 % of the E. coli density is observed. Thus, both samples lost their antibacterial ability after sterilisation (compare the luminescence with the uncoated control sample, shown in Fig. 10).
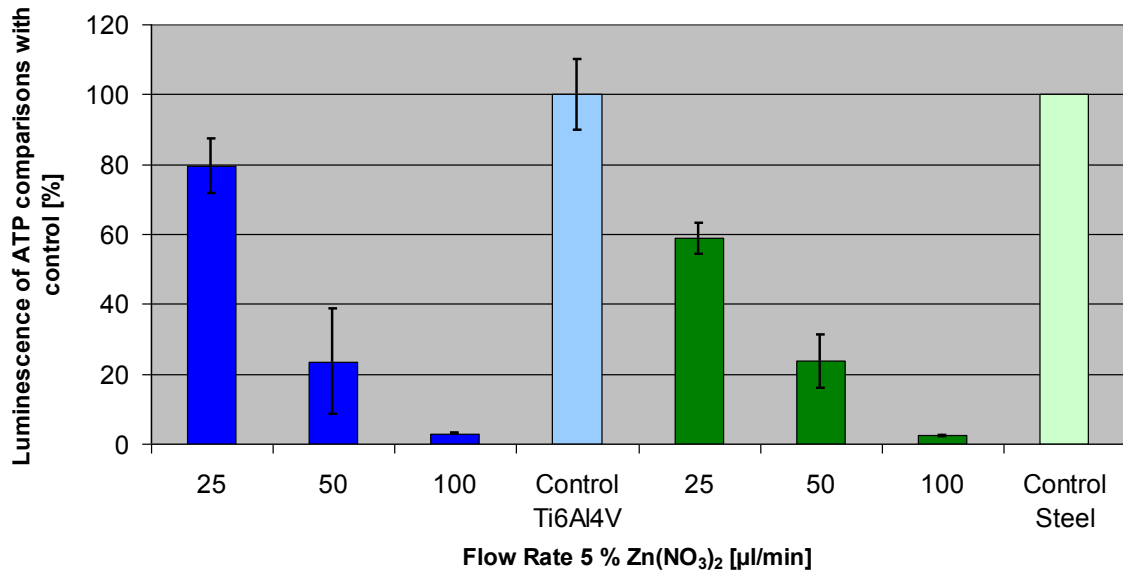
Figure. 9: *Influence of the secondary precursor flow rate of coated Zn-SiO$_x$ samples on detectable ATP, after 1000 washing cycles.*

Similarly to the Cu-SiO$_x$, a loss of the antibacterial ability was observed for the Zn-SiO$_x$ film. There, the increase of the luminescence after 15 and 30 cycles was, however, lower. The luminescence of the ATP of the coated Ti6Al4V substrates is about 120 % compared to 170 % for the stainless steel substrates.
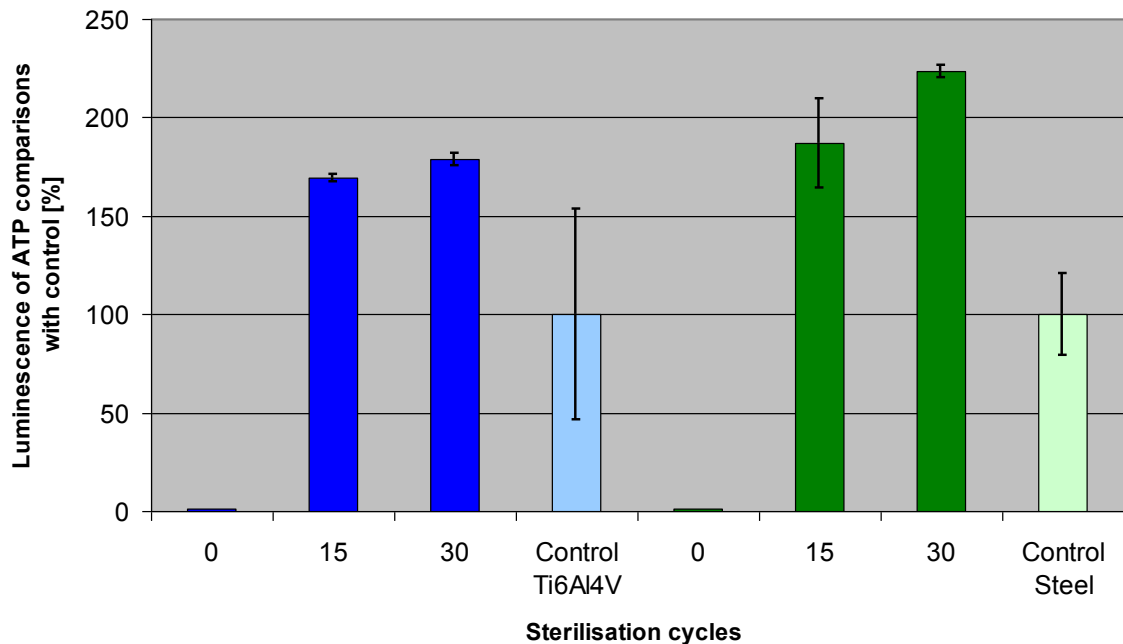

Figure 10: *Influence of the number of sterilisation cycles of coated Cu-SiO$_x$ samples grown at a secondary precursor flow rate of 50 µl/min on detectable ATP after 0, 15 and 30 sterilisation cycles.*

4 Discussion

Ag-SiO$_x$ has been demonstrated earlier [3] to be a promising candidate for antibacterial films for medical applications. However, Ag is a foreign element in the human body. Alternatively, antiseptic metals like Zn or Cu could be preferably used for medical implants, because they can be found as trace elements in the human body.

According to our current understanding, it appears that contact killing with Cu ions proceeds by successive membrane damage, Cu influx into the cells, oxidative damage, cell death and DNA degradation [10]. Zn ions are potent inhibitors of catabolism and O$_2$ metabolism. Zn ions also inhibits hydrogen peroxide production nearly completely but also enhances killing by peroxide added to cells [11,12].

Cu-SiO$_x$ and Zn-SiO$_x$ films exhibit a high particle density on the surface, which is related to the deposition process using the APCVD technique [6], and increases with increasing flow rate of the secondary precursor. The highest concentration of Cu and Zn was found in the particles. Their chemical state corresponds to CuO$_x$ or ZnO$_x$ and they are the dominant part of the film surface (see Figs. 1-3). A higher flow rate leads to a higher particle density, which correlates with a higher Cu and Zn fraction on the film surface. While the E. coli are exposed to the film surface, they are in direct contact with Cu and Zn ions, which leads to cell death (see Figs. 5-6). In this work, a functional gap for the Zn system was found (Fig. 5). With the secondary precursor concentration of 5 % and a flow rate of 100 µl/min, an antibacterial coating was deposited. With a flow rate of 25 µl/min, no antibacterial effect was obtained. Since the Cu doped films showed a stronger antibacterial effect, even if they were coated with lower secondary precursor concentration (2.5 %) and lower flow rates (12.5 µl/min), which correlates to the effective amount of antiseptic Cu, it is evident that Cu is more effective in contact killing of E coli than Zn.

The coatings did not show a cytotoxic effect (see Fig. 4), even if they have a pronounced antibacterial effect (Figs. 5-6). Independent of the tested flow rates, secondary precursors and substrates, a small inhibition in cell growth was observed within the first three days after exposure, but no cytotoxic effect was derived. A similar effect was also observed in experiments with Ag [5,13]. A possible explanation would be the quantitative release of antiseptic metal within a short period of time [4], which can efficiently kill bacteria, also affecting the growth of osteoblastic cells. In a previous work [6] it was shown that especially during the first ten washing cycles the loss of antiseptic material (Ag) from the film was relatively high. After this burst effect during the first cycles, the amount of the released Ag decreased only with a nearly linear function against tenfold multiplication steps of washing cycles.

The washability test leads to a huge change of the surface microstructure. Taking into account that most of the big particles are scrubbed from the surface, the concentration of Cu and Zn and thus the antibacterial ability is assumed to decreases dramatically. Nevertheless, a certain amount of Zn and Cu seems to be still homogenously distributed on the surface. This explains that the films show a slight antibacterial effect, even though washed about 1000 times (Fig. 8-9).

In a previous work [6] it was not possible to show antibacterial activity of one and the same sample if retested by repetitive interaction with the E. coli suspension. The main reason is that the procedure (sterilisation with ethanol for 1 h, washing with distilled water and ethanol, drying) is more stringent than the washing cycles and promotes a fast depletion of ions from the films. On the other hand, the surface could be sealed by the procedure inhibiting the release of Cu ions. It has been reported [14] that the contact killing efficiency of the Cu surface after the second soiling/cleaning cycle decreases. In a different study [15] the Cu surfaces remained active when soiled. From what is known about the mechanism of contact killing, it can be assumed that a clean Cu surface, free of oxide, wax, or other coating agents, will always be active in contact killing [10]. Another study [3] did not show any antibacterial activity after treatment at 500 °C using a muffle furnace. It seems that films are not resistant against heat, soil and washing procedures, which explains why the films lost their antibacterial functionality after sterilisation tests (see Fig. 10).

5 Conclusions

SiO_x films with a low, intermediate and high concentration of the alloying elements Cu and Zn, respectively, were synthesized by atmospheric pressure chemical vapour deposition and tested with respect to their antibacterial and cytotoxic effects. The best antibacterial ability was obtained for the CuO_x containing film with the highest Cu content of 0.2 at.%. While the Escherichia coli are exposed to the surface and killed within three hours, the mouse cells growth is just inhibited for the first three days. In order to have Zn-SiO_x films with the same antibacterial behaviour, the Zn concentration has to be in the range of 2.3 at.%. The films show sufficient antibacterial behaviour even after 1000 washing cycles; this is, however, limited after the sterilisation procedure.

Acknowledgments

References

1. Diegelmann RF, Evans MC. Wound healing: An overview of acute, fibrotic and delayed healing. Front. Biosci. 2004. p. 283–9.

2. Heidenau F, Mittelmeier W, Detsch R, Haenle M, Stenzel F, Ziegler G, Gollwitzer H. A novel antibacterial titania coating: metal ion toxicity and in vitro surface colonization. J. Mater. Sci. Mater. Med. 2005;16:883–8.

3. Zimmermann R, Pfuch A, Horn K, Weisser J, Heft A, Röder M, Linke R, Schnabelrauch M, Schimanski A. An Approach to Create Silver Containing Antibacterial Coatings by Use of Atmospheric Pressure Plasma Chemical Vapour Deposition (APCVD) and Combustion Chemical Vapour Deposition (CCVD) in an Economic Way. Plasma Process. Polym. 2011;8:295–304.

4. Stranak V, Wulff H, Rebl H, Zietz C, Arndt K, Bogdanowicz R, Nebe B, Bader R, Podbielski A, Hubicka Z, Hippler R. Deposition of thin titanium–copper films with antimicrobial effect by advanced magnetron sputtering methods. Mater. Sci. Eng. C. 2011;31:1512–9.

5. Ewald A, Glückermann SK, Thull R, Gbureck U. Antimicrobial titanium/silver PVD coatings on titanium. Biomed. Eng. Online. 2006;5:22.

6. Beier O, Pfuch A, Horn K, Weisser J, Schnabelrauch M, Schimanski A. Low Temperature Deposition of Antibacterially Active Silicon Oxide Layers Containing Silver Nanoparticles, Prepared by Atmospheric Pressure Plasma Chemical Vapor Deposition. Plasma Process. Polym. 2013;10:77–87.

7. Pfuch A, Horn K, Mix R, Ramm M, Heft A, Schimanski A. Direct and remote plasma assisted CVD at atmospheric pressure for the preparation of oxide thin films. Galvanotechnik. 2012;103:814–24.

8. C.D. WAGNER, J.F. MOULDER, L.E. DAVIS WMR. Handbook of X-ray photoelectron spectroskopy. Perking-Elmer Corporation, Physical Electronics Division; 1979.

9. Maroie S, Haemers G, Verbist JJ. Surface oxidation of polycrystalline α(75%Cu/25%Zn) and β(53%Cu/47%Zn) brass as studied by XPS: Influence of oxygen pressure. Appl. Surf. Sci. 1984;17:463–7.

10. Grass G, Rensing C, Solioz M. Metallic copper as an antimicrobial surface. Appl. Environ. Microbiol. 2011;77:1541–7.

11. Sheng J, Nguyen PTM, Marquis RE. Multi-target antimicrobial actions of zinc against oral anaerobes. Arch. Oral Biol. 2005;50:747–57.

12. Sawai J. Quantitative evaluation of antibacterial activities of metallic oxide powders (ZnO, MgO and CaO) by conductimetric assay. J. Microbiol. Methods. 2003;54:177–82.

13. Alt V, Khalilpour P, Wagener M, Domann E, Schnettler R. Ag/SiOxCy plasma polymer coating for antimicrobial protection of fracture fixation devices. Eur. Cells Mater. 2011. p. 6.

14. Airey P, Verran J. Potential use of copper as a hygienic surface; problems associated with cumulative soiling and cleaning. J. Hosp. Infect. 2007;67:271–7.

15. Wheeldon LJ, Worthington T, Lambert PA, Hilton AC, Lowden CJ, Elliott TSJ. Antimicrobial efficacy of copper surfaces against spores and vegetative cells of Clostridium difficile: the germination theory. J. Antimicrob. Chemother. 2008;62:522–5.